Overview of UPC Snowmass LoI physics cases

Mariusz Przybycień

AGH University of Science and Technology

Center for Frontiers in Nuclear Science
Workshop Series

RHIC Science Programs Informative
Toward EIC in the Coming Years

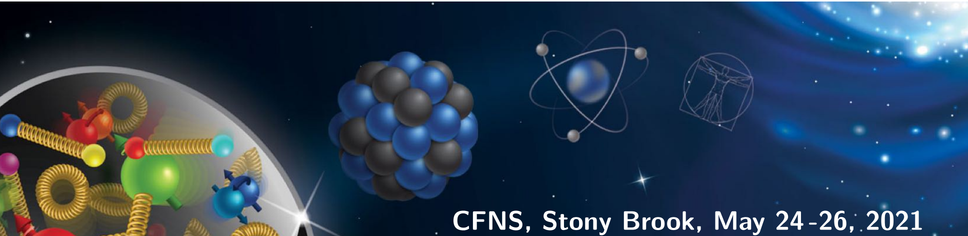

CFNS, Stony Brook, May 24-26, 2021

UPC Physics with Heavy-Ion Beams in Snowmass LoIs

Four UPC related LoIs have been submitted, to two EF study groups:

- EF07: QCD and strong interactions: Heavy Ions:
  - Ultra-Peripheral Collisions in Heavy-Ion Physics (70 references)

Jaroslav Adam[2], Carlos Bertulani[12], James D. Brandenburg[2], Frank Geurts[7], Victor P. Goncalves[5], Yoshitaka Hatta[2], Yongsun Kim[13], Spencer R. Klein[4], Cong Li[3], Wei Li[7], Michael Murray[6], Joakim Nystrand[9], Mariusz Przybycien[1,*], John P. Ralston[6], Christophe Royon[6], Lijuan Ruan[2], Bjoern Schenke[2], Janet Seger[10], Peter Steinberg[2], Daniel Tapia Takaki[6], Zebo Tang[11], Zhoudunming Tu[2], Ralf Ulrich[14], Ramona Vogt[4], Bowen Xiao[8], Zhangbu Xu[2,*], Shuai Yang[7], Wangmei Zha[11], Jian Zhou[3,*], and Ya-jin Zhou[3]

Ultraperipheral collisions (UPCs) of heavy ions at RHIC and LHC offer great opportunities to study strong field QED, EM/color charge fluctuations, collective phenomenon, electromagnetic properties of QGP, search BSM physics, and explore 3D nuclear structure with high luminosity beams of linearly polarized photons from Lorentz-boosted Coulomb field. Among these exciting directions of UPC studies, we select a few important new developments and emphasize on the polarization dependent effects in photon-photon processes and photon-nuclear interactions, and the processes as an electromagnetic probe of QGP properties.

  - Production of Charged BSM Particles at Future Heavy-Ion Colliders Via Photon-Photon Fusion

Authors: Laura Jeanty, Jenna Kishinevsky, Lawrence Lee

The Authors point out the possibility of the study of the production of ALP and other BSM particles in photon-photon fusion. Their plans include studies of the potential sensitivity of UPCs to higgsino and chargino production in different configurations of HI collisions, together with estimation of backgrounds.

  - New Phenomena Searches in Heavy Ion Collisions

Coordinators: Marco Drewes, David d'Enterria

In the part of the LoI related to UPC, the Authors outline possible measurements of particle production in photon-photon collisions, including new particles.

UPC Physics with Heavy-Ion Beams in Snowmass LoIs

- EF06: QCD and strong interactions: Hadronic structure and forward QCD:
  - New opportunities at the photon energy frontier (85 references)

Authors: Jaroslav Adam[9], Christine Aidala[40], Aaron Angerami[3], Benjamin Audurier[47], Carlos Bertulani[17], Christian Bierlich[24], Boris Blok[35], James Daniel Brandenburg[9], Stanley Brodsky[34], Aleksandr Bylinkin[2], Veronica Canoa Roman[42], Francesco Giovanni Celiberto[52], Jan Cepila[0], Grigorios Chachamis[46], Brian Cole[22], Guillermo Contreras[0], David d'Enterria[14], Adrian Dumitru[28], Arturo Fernández Téllez[20], Leonid Frankfurt[10,50], Maria Beatriz Gay Ducati[19], Frank Geurts[23], Gustavo Gil da Silveira[11], Francesco Giuli[26], Victor P. Goncalves[16] Iwona Grabowska-Bold[5], Vadim Guzey[12], Lucian Harland-Lang[32] Martin Hentschinski[29], T. J. Hobbs[25], Jamal Jalilian-Marian[28] Valery A. Khoze[15], Yongsun Kim[36], Spencer R. Klein[1], Simon Knapen[21], Mariola Kłusek-Gawenda[48], Michal Krelina[0], Evgeny Kryshen[12], Tuomas Lappi[38], Constantin Loizides[7], Agnieszka Luszczak[44], Magno Machado[39], Heikki Mäntysaari[38], Daniel Martins[7], Ronan McNulty[45], Michael Murray[2], Jan Nemchik[0], Jacquelyn Noronha-Hostler[33], Joakim Nystrand[6], Alessandro Papa[51], Bernard Pire[37], Mateusz Ploskon[1] Marius Przybycien[5], John P. Ralston[2], Patricia Rebello Teles[18] Christophe Royon[2], Björn Schenke[9], William Schmidke[9], Janet Seger[8], Anna Stasto[10], Peter Steinberg[9], Mark Strikman[10], Antoni Szczurek[48], Lech Szymanowski[31], Daniel Tapia Takaki[2], Ralf Ulrich[49], Orlando Villalobos Baillie[41], Ramona Vogt[3,4], Samuel Wallon[30], Michael Winn[43], Keping Xie[27], Zhangbu Xu[9], Shuai Yang[23], Mikhail Zhalov[12], and Jian Zhou[13]

Abstract: Ultra-peripheral collisions (UPCs) involving heavy ions and protons are the energy frontier for photon-mediated interactions. UPC photons can be used for many purposes, including probing low-x gluons via photoproduction of dijets and vector mesons, probes of beyond-standard-model processes, such as those enabled by light-by-light scattering, and studies of two-photon production of the Higgs.

Physics cases in Snowmass LoIs

- Photon-photon processes
  - Dilepton pairs production
    - explore the phase space of photon collisions in p_{T}, y and momentum-space-spin correlations in extreme QED fields,
    - explore strong EM fields; search for elusice Coulomb correction.
  - Dileptons as a probe in heavy ion collisions
    - using pure EM lepton pair production for studying EM properties of QGP,
    - correlations in dilepton pair production in non-UPC two-photon production,
  - Sensitive to many BSM processes including non-linear corrections to electromagnetism
    - LbyL - cross section is sensitive to all charged particles, including BSM particles such as vector fermions, GeV- mass axion-like particles (ALPs) and magnetic monopoles.
    - Limits on anomalous quartic gauge couplings.
- Photon-nucleus/nucleon interactions:
  - Linearly polarized photon-gluon collisions
    - imaging gluon momentum and space distributions in nuclei using photoproduction of VMs,
    - using polarization dependent observables (e.g. azimuthal modulation and its p_{T} dependence).
  - Photoproduction in non-UPC heavy-ion collisions
    - photoproduction of J/ψ at low p_{T} accompanying hadronic collisions in QGP.
  - Ultraperipheral p+A collisions
    - using exclusive diffractive dijet production to constrain the gluon Wigner distribution,
    - using polarized protons to access GPD E_g.

Ultra-peripheral heavy-ion collisions at RHIC and LHC

- Ultrarelativistic heavy-ions produce highly Lorentz contracted electromagnetic fields.
- Weizsäcker-Williams Equivalent Photon Approximation (EPA) - these electromagnetic fields can be treated as fluxes of coherent (virtual) photons with ($R_{\mathrm{A}} = 7$ fm):

$$Q^2 < (\hbar/R_{\mathrm{A}})^2 \approx 10^{-3}\ \mathrm{GeV}^2$$

- Ultra-Peripheral Collision (UPC): $\boldsymbol{b > 2R_{\mathrm{A}}}$
  - hadronic interactions are strongly suppressed,
  - intense sources of photons ($\propto Z^2$),
  - maximum energy of coherent photons:

    Au+Au at $\sqrt{s_{\mathrm{NN}}} = 200$ GeV:

    $E_\gamma = \gamma\hbar c/R_{\mathrm{A}} = \{\gamma \approx 106.6\} \approx 3$ GeV

    Pb+Pb at $\sqrt{s_{\mathrm{NN}}} = 5.02$ TeV:

    $E_\gamma = \gamma\hbar c/R_{\mathrm{A}} = \{\gamma \approx 2676\} \approx 75$ GeV

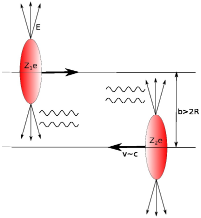

arXiv:1910.12400 [nucl-ex]

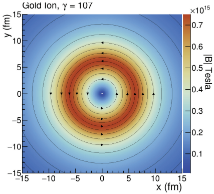

- UPCs of HIs allow to study:
  - two-photon interactions (direct production of fermion or boson pairs, tests of QED under extreme conditions, search for new physics, ...),
  - photonuclear production (VM production, hadronic final states, ...).

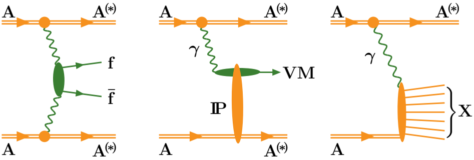

Two-Photon Collisions

Two-photon collisions formalism

- Cross section for two-photon production of final state X with mass W: (Baltz et al., Phys. Rep. 458 (2008) 1; S. Klein et al., Ann. Rev. 70 (2020) 323 and PRD102, 094013 (2020)):

$$\sigma(AA \to AA + X) = \iint \frac{dk_1}{k_1}\frac{dk_2}{k_2} n(k_1) n(k_2) \sigma(\gamma\gamma \to X(W))$$

where $n(k)$ is the flux of photons of energy k.

- The equivalent two-photon luminosity is the convolution of equivalent photon spectra from the two nuclei in the impact parameter $\vec{b}$ space:

$$\frac{d^2\mathcal{L}_{\gamma\gamma}}{dW\,dy} = \mathcal{L}_{AA}\frac{W}{2}\iint_{b_1,b_2>R} d^2b_1\, d^2b_2\, n(k_1,b_1) n(k_2,b_2) P(b)[1-P_H(b)], \qquad b = |\vec{b}_1 - \vec{b}_2|$$

where $P_H(b)$ is the hadronic interaction probability and $P(b)$ is the total breakup condition.

- Nuclear photon flux: $n(k,b) = \frac{\mathrm{d}^3N}{\mathrm{d}k\,\mathrm{d}^2b} = \frac{Z^2\alpha k}{\pi^2\beta^2\gamma^2}\left[K_1^2(x) + \frac{1}{\gamma^2}K_0^2(x)\right]$, where $x = bk/\beta\gamma$

- CMS energy W and rapidity $y = \frac{1}{2}\ln\left(\frac{k_1}{k_2}\right)$ are determined by photons' energies $k_{1,2} = \frac{W}{2}e^{\pm y}$

- The cross section for two-photon lepton pair production: $\frac{\mathrm{d}^2\sigma}{dW\,dy} = \frac{d^2\mathcal{L}_{\gamma\gamma}}{dW\,dy} \times \sigma(\gamma\gamma \to \ell\ell)$

where (here M is the mass of the lepton ℓ)

$$\sigma_{\gamma\gamma} = \frac{4\pi\alpha^2}{W^2}\left[\left(2 + \frac{8M^2}{W^2} - \frac{16M^4}{W^4}\right)\ln\frac{W+\sqrt{W^2-4M^2}}{2M} - \sqrt{1-\frac{4M^2}{W^2}}\left(1+\frac{4M^2}{W^2}\right)\right]$$

Exclusive dimuon pairs production in ATLAS

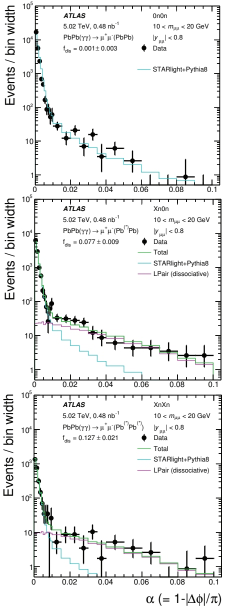

arXiv:2011.12211 [nucl-ex]

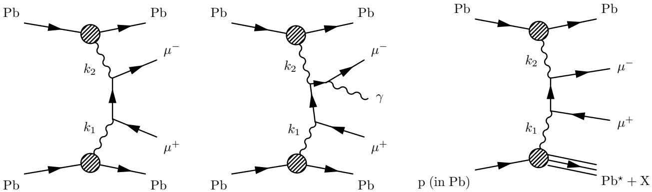

- ATLAS data: Pb+Pb collisions at $\sqrt{s_{\rm NN}} = 5.02$ TeV, $\mathcal{L} = 480$ μb^{-1}
- Signal includes: Breit-Wheeler process and higher order final state.
- Dissociative bkgr. (non-EPA process) is modeled and removed.
- Signal: $p_{\rm T,\mu} > 4$ GeV, $|\eta_\mu| < 2.4$, $m_{\mu\mu} > 10$ GeV, $p_{\rm T,\mu\mu} < 2$ GeV
- MC signal: STARlight 2.0 + Pythia8 (to add FSR calculations).

  MC dissociative bkgr: LPair 4.0 (including nuclear breakup).
- Remove dissociative bkgr. from $\gamma\gamma \to \mu\mu$ where one photon comes from Pb ($p_{\rm T} \sim 25$ MeV) and other (harder) from a nucleon from the other Pb ion, using template fits to acoplanarity ($\alpha = 1 - |\Delta\phi|/\pi$):
  - no significant diss. bkgr. in $0n0n$ selection,
  - ${\rm X}n0n$ and ${\rm X}n{\rm X}n$ have diss. contributions at 7% and 12% levels.

Exclusive dimuon pairs production in ATLAS

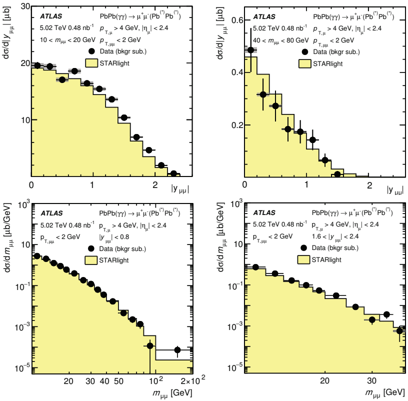

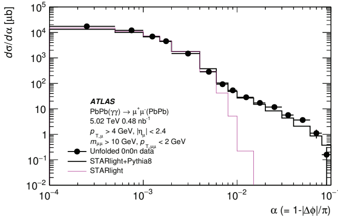

arXiv:2011.12211 [nucl-ex]

- Differential cross sections measured as functions of: $m_{\mu\mu}$, $y_{\mu\mu}$, $\cos\theta^{\star}_{\mu\mu}$, α and $k_{\min,\max}$.
- Generally well described by STARlight 2.0 - some increase in data observed at higher $y_{\mu\mu}$.
- A difference in shape for $\alpha < 0.01$ could be explained by a small change in the p_{T} spectrum assumed by STARlight.
- Incoming photon energies estimated for $p_{\mathrm{T}} \sim 0$:

  $$k_{1,2} = (m_{\mu\mu}/2)\exp\left[\pm y_{\mu\mu}\right]$$

  Requirement of $b > R_{1,2}$ in two-photon flux.
- Total fiducial cross section: $\sigma^{\mu\mu}_{\mathrm{fid}} = 34.1 \pm 0.3(\mathrm{stat}) \pm 0.7(\mathrm{sys})$

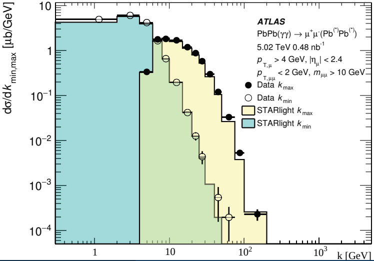

Non-exclusive dimuon pairs production in ATLAS

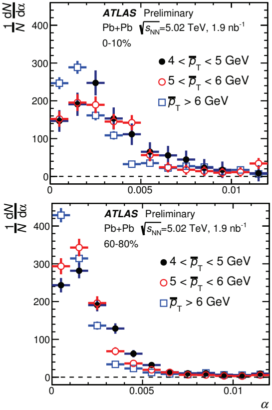

- ATLAS data: Pb+Pb at $\sqrt{s_{\mathrm{NN}}} = 5.02$ TeV, $\mathcal{L} = 1.9$ nb^{-1}
- Signal: non-exclusive, non-ultra-peripheral muon pairs produced in $\gamma\gamma$ collisions (first observation: PRL 121, 212301 (2018)).
- Cuts to remove bkgr. from dileptons from heavy flavour decays:
  - acoplanarity, $\alpha = 1 - |\Delta\phi|/\pi < 0.012$,
  - p_{T} imblance of the pair, $A \equiv (p_{\mathrm{T1}} - p_{\mathrm{T2}})/(p_{\mathrm{T1}} + p_{\mathrm{T2}}) < 0.08$,
  - impact parameter: $d_{0\mathrm{pair}} < 0.1$ mm, $z_{0\mathrm{pair}} < 0.2$ mm.
- Modest peaks develop in α as collisions get more central.
- Perpendicular transverse momentum:
  $k_{\perp} \equiv (p_{\mathrm{T1}} + p_{\mathrm{T2}})|(\pi - \Delta\phi)|/2 = \pi\alpha\bar{p}_{\mathrm{T}}$
- Sharper peaks are observed in $k_{\perp}$, which scale with p_{T}.

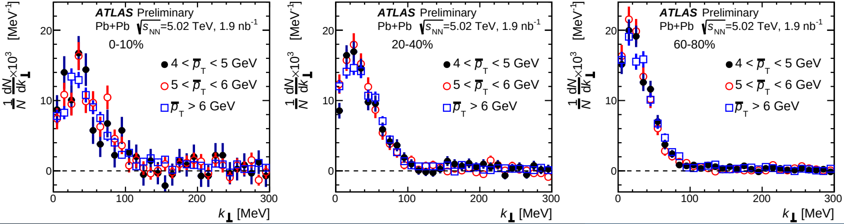

ATLAS-CONF-2019-051

Non-exclusive dimuon pairs production in ATLAS

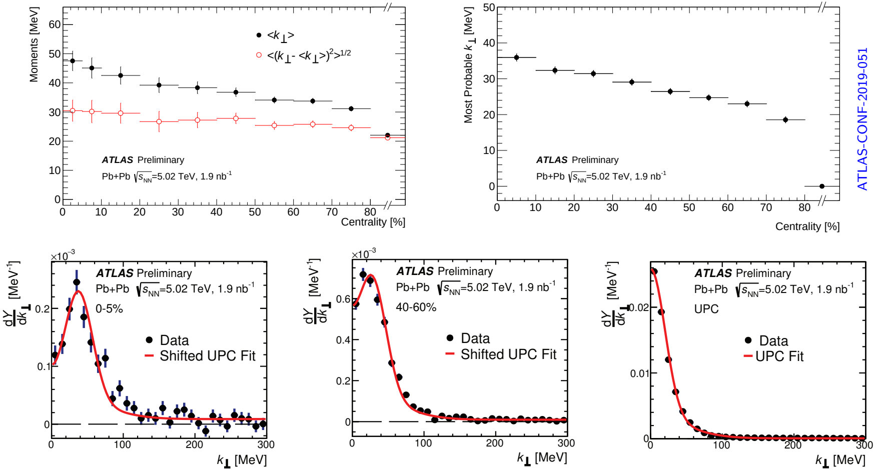

- Clear increase in $\langle k_\perp \rangle$ and a weaker in RMS, from peripheral to central events, is seen in data.
- Phenomenological fits to $k_\perp$ distributions are performed to provide an estimate of the peak position.
- Transverse momentum broadening predicted in Zha, et al. PLB 800 (2020) 135089, by including the impact parameter dependence of the initial photon p_{T} in QED calculations.

Non-exclusive dielectron pairs production in STAR

PRL 121, 132301 (2018)

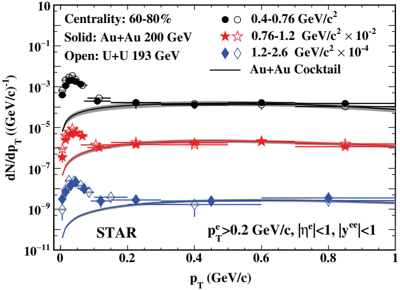

- STAR data: Au+Au collisions at $\sqrt{s_{\rm NN}} = 200$ GeV and U+U collisions at $\sqrt{s_{\rm NN}} = 193$ GeV.
- Signal: Inclusive e^+e^- pairs with $p_{\rm T}^e > 0.2$ GeV$/c$, $|\eta^e| < 1$, $|y^{ee}| < 1$.
- Observation of an excess of the number of e^+e^- pairs over the hadronic cocktail for events with $p_{\rm T}^{ee} < 0.15$ GeV$/c$, more significant in paripheral $(60-80\%)$ than in central $(10-40\%)$ events.
- After subtraction of the hadronic cocktail, the $p_\perp^2$ distributions in data are well described by the Zha, et al. PLB 800 (2020) 135089 prediction.

PLB 800, 135089 (2020)

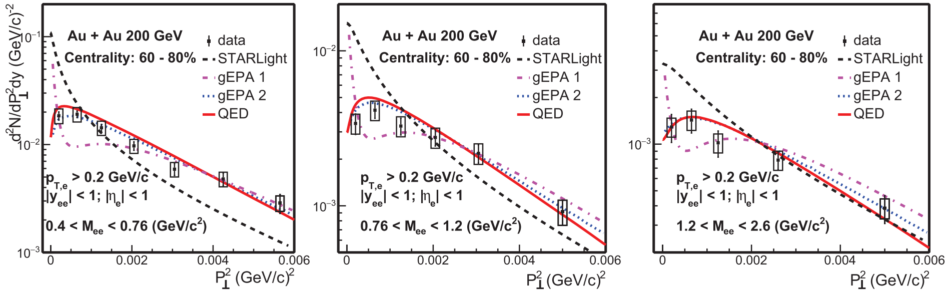

Dimuon accoplanarity and forward neutron multiplicity

- CMS data: Dimuon pairs production in UPC of Pb+Pb at $\sqrt{s_{\rm NN}} = 5.02$ TeV, $\mathcal{L} = 1.5$ nb^{-1}.
- Each α spectrum consists of a narrow core, $\alpha \sim 0$, (from the LO $\gamma\gamma$ scattering) and a long tail (HO $\gamma\gamma$ processes, e.g., FSR from the produced lepton(s), multiple-photon interactions).
- The tail contribution becomes larger when going form $0n0n$ to $\mathrm{X}n\mathrm{X}n$ topology.
- To quantify this one can fit α distributions with a two-component empirical function.
- Strong neutron multiplicity dependence of α^{core} and $\langle m_{\mu\mu}\rangle$.
- Initial photons producing $\mu^+\mu^-$ pairs have a significant b dependence of their $p_{\rm T}$, which impacts the $p_{\rm T}$ and acoplanarity of muon pairs in the final state.

arXiv:2011.05239 [hep-ex]

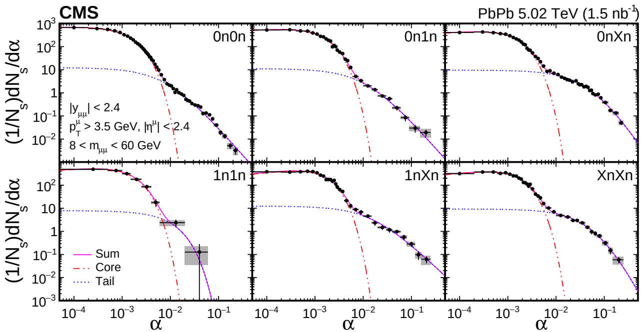

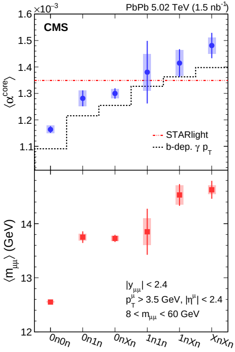

Production of dielectron pairs in UPC in STAR

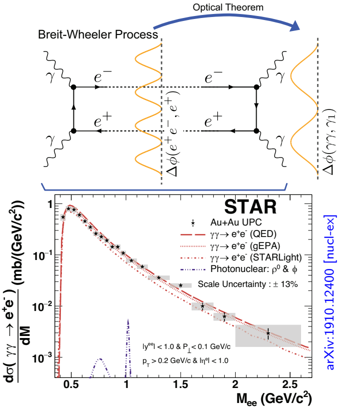

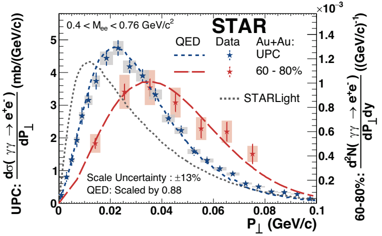

- STAR data: Exclusive e^+e^- pairs in Au+Au UPC at $\sqrt{s_{NN}} = 200$ GeV, $\mathcal{L} = 700$ μb^{-1}.
- Breit-Wheeler process and the related LbyL scattering, but are predicted to differ in angular distribution due to the initial photon polarization.
- No vector mesons in the mass spectrum - forbidden by selection rules for real photons with helicity ± 1.
- Measured fiducial cross section:

$$\sigma^{\text{fid}}_{\gamma\gamma\rightarrow e^+e^-} = 261 \pm 4(\text{stat}) \pm 13(\text{sys}) \pm 34(\text{scale})\ \mu\text{b}^{-1}$$

In a good agreement with theory predictions $\sigma_{\text{gEPA}} = 260$ μb^{-1} (Zha et al., PLB 800 (2020) 135089)

- Distributions of the pair transverse momentum, $P_\perp$, show clear dependence of the process on the initial geometry (b).
- Leading order QED calculation of the process describes both spectra.
- Impact parameter dependence of the photons k_T was confirmed byc CMS (previous slide).

Collisions of linearly polarized photons

- Prediction of $\cos 4\Delta\phi$ modulation for $\gamma\gamma \to e^+e^-$ process in case of linear polarization of the colliding photons, where $\Delta\phi$ is the azimuthal angle between the vectors $(p_T^{e^+} + p_T^{e^-})$ and $p_T^{e^+}$ (Li et al., PLB 795, 576 (2019))
- Results of the fit of the function $f(\Delta\phi) = C(1 + A_{2\Delta\phi}\cos 2\Delta\phi + A_{4\Delta\phi}\cos 4\Delta\phi)$:

Differential Quantities	Ultra-Peripheral				Peripheral	
	Measured	QED	SuperChic	STARLight	Measured	QED
$\lvert A_{4\Delta\phi}\rvert$ (%)	16.8 ± 2.5	16.5	19	0	27 ± 6	34.5
$\lvert A_{2\Delta\phi}\rvert$ (%)	2.0 ± 2.4	0	5	5	6 ± 6	0

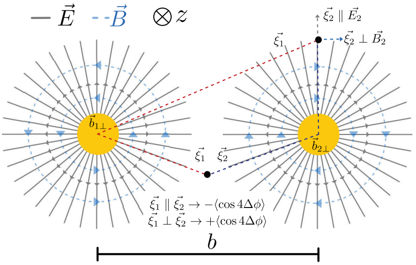

PLB 800 (2020) 135089

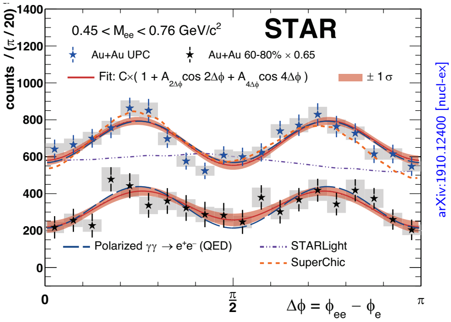

Light-by-light scattering in ATLAS and CMS

- Measured process (at $\sqrt{s_{\mathrm{NN}}} = 5.02$ TeV):

  $\mathrm{Pb} + \mathrm{Pb}(\gamma^{\star}\gamma^{\star}) \to \mathrm{Pb}^{(\star)} + \mathrm{Pb}^{(\star)} + \gamma\gamma$

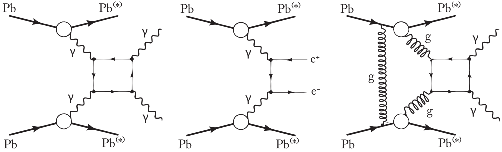

- Data: $\mathcal{L} = 2.2$ nb^{-1} (ATLAS)

  $\mathcal{L} = 0.39$ nb^{-1} (CMS)

- Fiducial cuts ($A_\phi = 1 - |\Delta\phi|/\pi$):

  ATLAS: $E_T^\gamma > 2.5$ GeV, $|\eta^\gamma| < 2.37$, $m_{\gamma\gamma} > 5$ GeV, $p_T^{\gamma\gamma} < 1$ GeV, $A_\phi < 0.01$

  CMS: $E_T^\gamma > 2$ GeV, $|\eta^\gamma| < 2.4$, $m_{\gamma\gamma} > 5$ GeV, $p_T^{\gamma\gamma} < 1$ GeV, $A_\phi < 0.01$

- MC simulation:

  Signal: Box diagram ($\ell^+\ell^- + q\bar{q} + (W^\pm)$) - SuperChic 3.0 (ATLAS) and MadGraph 5 (CMS),

  Background: STARLIGHT 2.0 for $\gamma\gamma \to e^+e^-$ and SuperChic 3.0 for CEP ($gg \to \gamma\gamma$).

- Both ATLAS and CMS data are well described by the MC predictions.

JHEP 03, 243 (2021)

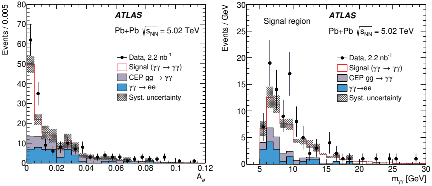

PLB 797, 134826 (2019)

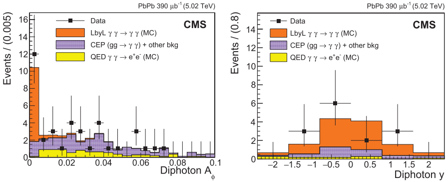

Search for ALPs in LbyL scattering in ATLAS and CMS

- ATLAS measured several fiducial differential and the total cross sections:

  $\sigma_{\mathrm{fid}} = 120 \pm 17$ (stat) ± 13 (sys) ± 4 (lumi) nb

  Prediction from SuperChic 3.0: $\sigma_{\mathrm{fid}} = 78 \pm 8$ nb
- The data-to-theory ratio is 1.50 ± 0.32.

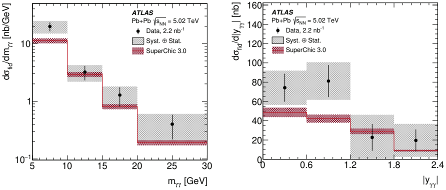

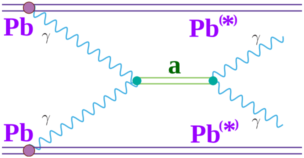

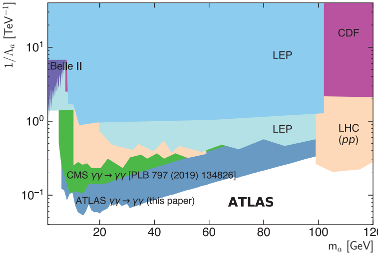

- Any particle coupling directly to photons could be produced in s-channel process in $\gamma\gamma$ collisions, leading to a resonance peak in the invariant mass spectrum.
- The measured $m_{\gamma\gamma}$ distribution is used to search for possible narrow diphoton resonances, e.g. pseudoscalar ALPs produced in the process $\gamma\gamma \to a \to \gamma\gamma$.
- In this study, LbyL, QED and CEP are backgrounds.
- The measured $m_{\gamma\gamma}$ is used to set upper limits at the 95% CL on the ALP production cross section in the process $\gamma\gamma \to a \to \gamma\gamma$ and also on the ALP coupling to photons $(1/\Lambda_a)$.
- ATLAS set the best exclusion limits so far over the mass range of $6 < m_a < 100$ GeV.

Coherent Diffractive Vector Meson Production

Diffractive photoproduction of vector mesons in UPC

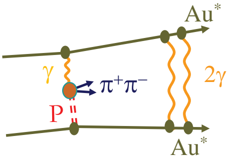

- Coherent diffractive photoproduction of ρ^0 mesons:

$$\mathrm{Au} + \mathrm{Au} \rightarrow \mathrm{Au}^{\star} + \mathrm{Au}^{\star} + \rho^0$$

- Cross section integrated over impact parameter:

$$\sigma(A_1 A_2 \rightarrow A_1^{\star} A_2^{\star} \rho^0) = \iint \mathrm{d}^2 b\, P_1(b, A^{\star}) P_2(b, A^{\star}) P(b, \rho^0)[1 - P_{\mathsf{Had}}(b)]$$

- $\pi^+\pi^-$ invariant mass spectrum can be well fitted by the sum of BW shapes for ρ^0 and ω, direct $\pi^+\pi^-$ production and their interference terms:

$$\frac{d\sigma}{dM_{\pi^+\pi^-}} \propto \left| A_\rho \mathrm{BW}_\rho + C_\omega e^{i\phi_\omega} \mathrm{BW}_\omega + B_{\pi\pi} \right|^2, \qquad \mathrm{BW_v} = \frac{\sqrt{M_{\pi\pi} M_{\mathrm{v}} \Gamma_{\mathrm{v}}}}{M_{\pi\pi}^2 - M_{\mathrm{v}}^2 + i M_{\mathrm{v}} \Gamma_{\mathrm{v}}}$$

- Coherent heavy VM photoproduction is sensitive to the gluon distribution in the target, and thus to the gluon shadowing effects (e.g. saturation) at small Bjorken-x.
- Mass of a heavy VM, m_{V}, sets the scale, $Q^2 \sim m_{\mathrm{V}}^2/4$, corresponding to the regime of pQCD.
- Bjorken-x of the gluonic exchange and the per nucleon $\gamma\mathrm{A}$ energy squared, $W_{\gamma\mathrm{A}}^2$ are related to the rapidity of the coherently produced VM ($\pm$ signs indicate that either of the incoming ions can be the source of the photon):

$$x = (m_{\mathrm{V}}/\sqrt{s_{\mathrm{NN}}}) \exp(\pm y) \qquad W_{\gamma\mathrm{A}}^2 = 2 E_{\mathrm{N}} m_{\mathrm{V}} \exp(\pm y)$$

Diffractive photoproduction of ρ^0 mesons in STAR

- STAR data: Photoproduction of $\pi^+\pi^-$ pairs in Au+Au UPC at $\sqrt{s_{NN}} = 200$ GeV
- Invariant mass spectrum is well fitted by the sum of ρ^0 and ω mesons and direct $\pi^+\pi^-$ pairs.
- $d\sigma/dy$ cross section is measured for (XnXn) and (1n1n) topologies.

  Assymetry between positive and negative rapidity reflects the rapidity-dependent systematic uncertainties due to detector (TOF) and does not apply to rapidity-integrated measurements.

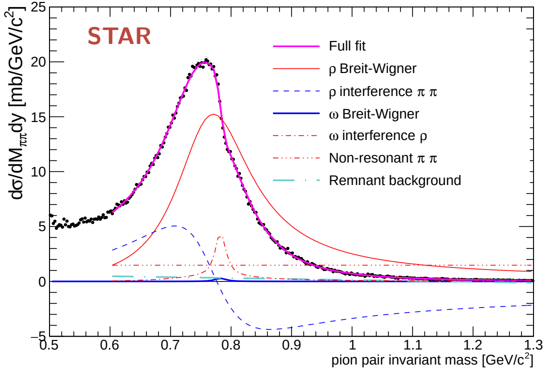

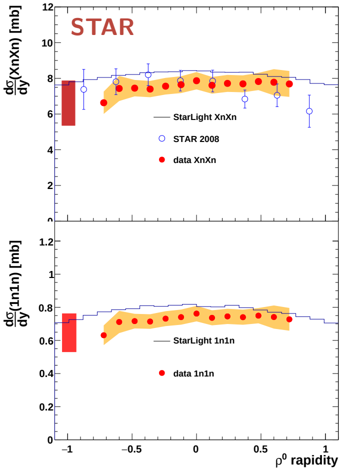

Diffractive photoproduction of ρ^0 mesons in STAR

- $d\sigma/dt$ for ρ^0 production is measured within $|y| < 1$, for both (XnXn) and (1n1n) topologies.
- Coherent spectrum of $d\sigma/dt$ is obtained by subtracting incoherent part from the full spectrum (estimated from fit of dipole form factor $F(t) = A/(Q_0^2 + |t|)^2$ in the range $-t > 0.2$ GeV^2).
- Clear diffractive minima can be seen - gold nuclei appear to be acting like black discs.
- Transverse density distribution of the Au nuclei can be determined with 2D Fourier transform of the coherent $d\sigma/dt$. The radial distribution can be obtained with Hankel transformation:

$$F(b) \propto \frac{1}{2\pi} \int_0^\infty dp_\mathrm{T}\, p_\mathrm{T} J_0(bp_\mathrm{T}) \sqrt{\frac{d\sigma}{dt}}$$

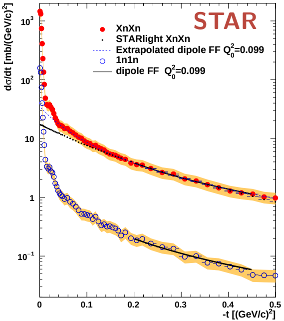

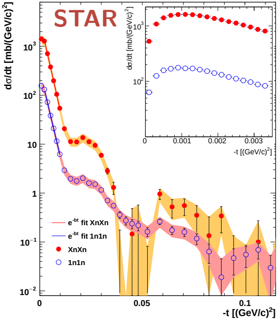

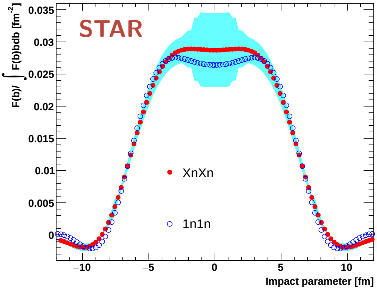

Diffractive production of ρ^0 mesons in ALICE

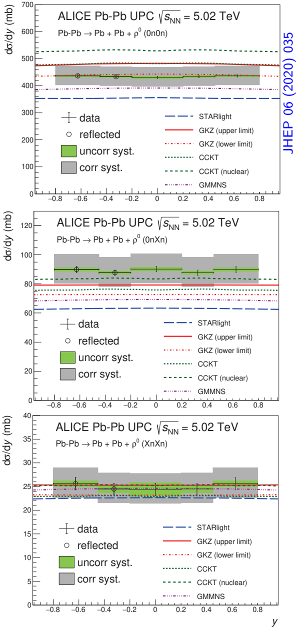

- ALICE data: exclusive $\rho(770)^0$ photoproduction in UPC of Pb+Pb at $\sqrt{s_{\rm NN}} = 5.02$ TeV and Xe+Xe at $\sqrt{s_{\rm NN}} = 5.44$ TeV
- The cross sections $d\sigma/dy$ are measured in the range $|y| < 0.8$ for three nuclear breakup classes: (0n0n), (0nXn), (XnXn)
- In case of Xe+Xe cross section, the measured fractions of the three nuclear breakup classes roughly equal to: $90.5\%, 8.5\%, 1.0\%$
- The measured cross sections are compared with predictions based on different models of nuclear shadowing.
- The measured UPC cross sections have been converted to $\sigma_{\gamma A}$ by dividing by $2\times$ corresponding photon flux.
- The dependence of $\sigma_{\gamma A}$ obtained at $W_{\gamma A,n} = 65$ GeV, for $A = p, \mathrm{Xe}, \mathrm{Pb}$ on mass number A is fitted with a power-law model $\sigma_{\gamma A} = \sigma_0 A^\alpha$ and compared other theory predictions.

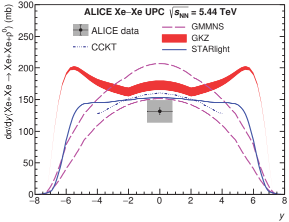

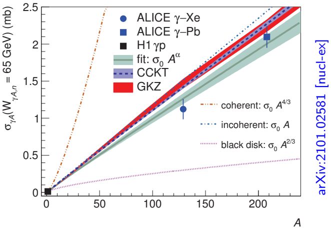

Diffractive production of ρ^0 mesons in CMS

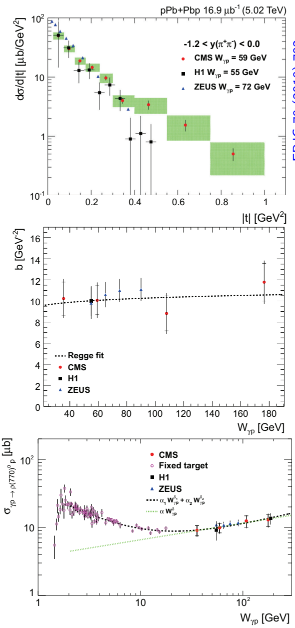

EPJC 79 (2019) 702

- CMS data: p+Pb at $\sqrt{s_{\rm NN}} = 5.02$ TeV ($E_p = 4$ TeV, $E_{{\rm Pb}/N} = 1.58$ TeV), $\mathcal{L} = 7.4\ \mu{\rm b}^{-1} + 9.6\ \mu{\rm b}^{-1}$
- Signal: exclusive production of $\rho(770)^0 \to \pi^+\pi^-$ in UPC
- STARlight 2.2 used for signal and background (non-resonant production of $\pi^+\pi^-$) simulation, and also for $W_{\gamma p}$ estimation.
- Differential cross section $d\sigma/d|t|$ has been measured for $|y(\pi^+\pi^-)| < 2$ and $p_{\rm T}(\pi^+\pi^-) > 0.15$ GeV.
- $d\sigma/d|t|$ measured in the range $-1.2 < y(\pi^+\pi^-) < 0$ is in a good agreemnt with HERA results.
- The slope parameters b extracted from the exponential fits $A\exp\left[-bt + ct^2\right]$ to $d\sigma/d|t|$ are compared to HERA results.
- For the integrated rapidity range $|y(\pi^+\pi^-)| < 2$ the fit gives:

  $b = 9.2 \pm 0.7({\rm stat})\ {\rm GeV}^{-2}$ and $c = 4.6 \pm 1.6({\rm stat})\ {\rm GeV}^{-4}$
- Fit of the Regge formula $b = b_0 + 2\alpha' \ln\left(W_{\gamma p}/W_0\right)^2$

  to the CMS data only gives α' consistent with HERA results:

  $$\alpha' = 0.28 \pm 0.11({\rm stat}) \pm 0.12({\rm sys})$$
- The resulting photon-proton cross sections, $\sigma(\gamma p \to \rho^0 p)$, are ploted vs $W_{\gamma p}$ and compared to previous measurements and fitted with the formula $\sigma = \alpha_1 W_{\gamma p}^{\delta_1} + \alpha_2 W_{\gamma p}^{\delta_2}$.

Diffractive photoproduction of J/ψ mesons in ALICE

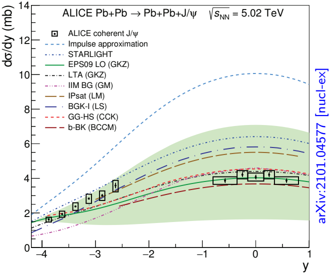

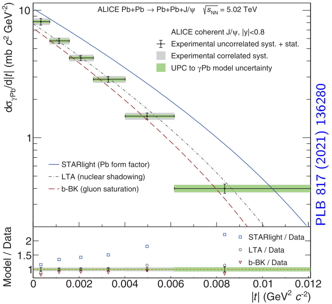

- ALICE data: Coherent photoproduction of $J/\psi \to \mu^+\mu^-$ in Pb+Pb UPC at $\sqrt{s_{\rm NN}} = 5.02$ TeV
- ALICE measured $d\sigma/dy$ in forward $(-4 < y < -2.5)$ and mid-rapidity $(|y| < 0.8)$ ranges.
- Forward rapidity range corresponds to a Bjorken-x either in the range $x \in (1.1, 5.1) \times 10^{-5}$ or $x \in (0.7, 3.3) \times 10^{-2}$ depending on which nucleus emitted the photon.
  - Models: $(x \sim 10^{-2})$ is dominant at forward rapidities and ranges from 60% at $y = -2.5$ to 95% at $y = -4$.
- The mid-rapidity corresponds to $x \in (0.3, 1.4) \times 10^{-3}$
- Measured cross sections are compatible with models predicting shadowing of about 65%.
- The cross section for the coherent production of J/ψ at mid-rapidity and in bins of $p_{\rm T}^2$ was converted to the $\gamma{\rm Pb}$ cross section as a function of $|t|$ using the formula:

$$\left.\frac{d^2\sigma^{\rm coh}_{J/\psi}}{dy\, dp_{\rm T}^2}\right|_{y=0} = 2n_{\gamma{\rm Pb}}(y=0)\,\frac{d\sigma_{\gamma{\rm Pb}}}{d|t|}, \qquad |t| \approx p_{\rm T}^2$$

- The $|t|$-dependent cross section is also better reproduced by models including shadowing (GSZ) or gluon-saturation effects from b-dependent BK equation than by STARlight.

Diffractive photoproduction of J/ψ mesons in p+Pb

- ALICE data: Coherent exclusive photoproduction of $\gamma p \to J/\psi + p$ in p+Pb UPC at $\sqrt{s_{\rm NN}} = 5.02$ TeV ($E_p = 4$ TeV, $E_{{\rm Pb}/N} = 1.58$ TeV)
- J/ψ is reconstructed in two decay channels $J/\psi \to \ell^+\ell^-$ $(\ell = e, \mu)$.
- Cross section as a function of the rapidity of J/ψ was measured in the range $-2.5 < y < 2.7$, corresponding to $40 < W_{\gamma p} < 550$ GeV.
- $\sigma(\gamma + p \to J/\psi + p)$ was obtained from $d\sigma/dy$ using relation: $\dfrac{d\sigma}{dy} = k\dfrac{dn}{dk}\sigma(\gamma + p \to J/\psi + p)$

  where $k = (M_{J/\psi}/2)\exp(-y)$ is the photon energy in LAB, and $k\,dn/dk$ is the photon flux.
- The ALICE results together with similar measurements from other experiments cover the range $24 < W_{\gamma p} < 706$ GeV corresponding to $2 \times 10^{-5} < x < 2 \times 10^{-2}$

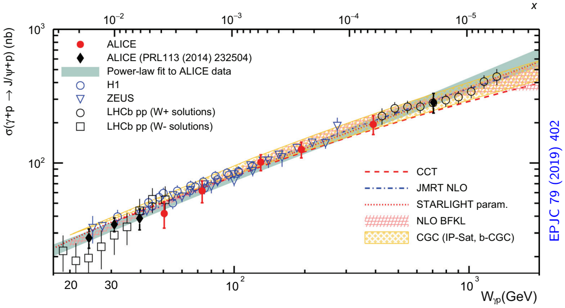

- Cross sections measured by different experiments are in agreement between each other and with all model predictions.
- ALICE measurement is consistent with a power-law dependence $\sim W_{\gamma p}^{\delta}$ with $\delta = 0.70 \pm 0.05$.
- There is no sign of gluon saturation effects.

Diffractive production of Υ mesons

- CMS data: Coherent exclusive photoproduction of $\gamma p \rightarrow \Upsilon(\mathrm{nS})p$, $(n = 1, 2, 3)$ in p+Pb UPC at $\sqrt{s_{\mathrm{NN}}} = 5.02$ TeV ($E_p = 4$ TeV, $E_{\mathrm{Pb}/N} = 1.58$ TeV), $\mathcal{L} = 32.6$ nb^{-1}
- The cross section for the production of $\Upsilon(\mathrm{nS})$ is measured in the range $|y| < 2.2$ as a function of p_{T}^2 and y.
- p_{T}^2-differential cross section is fitted with exponential - $b = 6.0 \pm 2.1(\mathrm{stat}) \pm 0.3(\mathrm{sys})$ GeV^{-2}
- $d\sigma_{\Upsilon(1S)}/dy$ is converted to $\sigma(\gamma p \rightarrow \Upsilon(1S)p)$ as a function of $W_{\gamma p}$ and compared with other measurements.
- $\sigma(\gamma p \rightarrow \Upsilon(1S)p)$ follows a power-law energy dependence, $\sim (W_{\gamma p}\,[\mathrm{GeV}]/400)^{\delta}$.

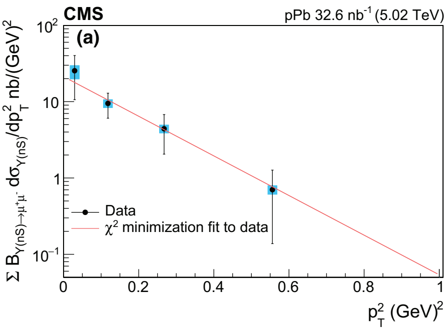

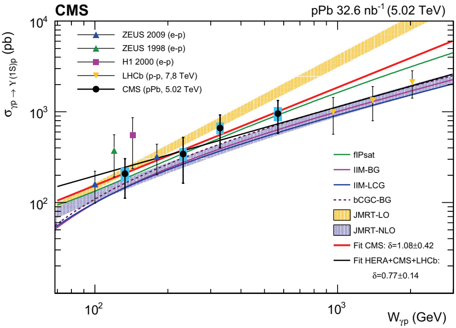

EPJC 79 (2019) 277

Photonuclear Production of Dijets

Dijets production in UPC in ATLAS

- ATLAS data: Pb+Pb at 5.02 TeV, 380 μb^{-1}; trigger: ZDC (0nXn) + jet
- Due to large Lorentz boost energetic (up to ~ 75 GeV) coherent photons can produce dijets in photonuclear processes with sufficient rates to provide a way to study nPDF.
- Virtual photons emitted by a nucleus can interact through direct or resolved processes with partons in the other nucleus.
- Due to no color exchange between the dijet system and the nucleus which emitted the photon, no significant particle production is expected in the rapidity region between the them. Also coherently emitted photons do not excite significantly the source nucleus.

- Rapidity gap:
  $\Sigma_{\gamma}\Delta\eta > 2$
  $\Sigma_{\mathrm{A}}\Delta\eta < 3$
- Jet requirements:
  anti-k_{T}, $R = 0.4$
  $p_{\mathrm{T}} > 15$ GeV,
  $|\eta| < 4.4$
  Two or more jets are required in an event; at least one with $p_{\mathrm{T}} > 20$ GeV.
  $m_{\text{jets}} > 35$ GeV

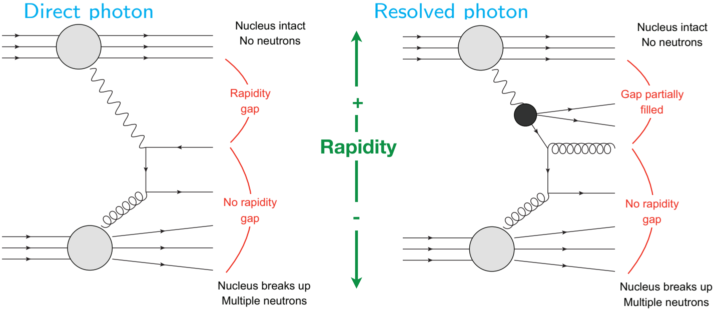

Dijets production in UPC in ATLAS

- Kinematical variables used in the measurement (i runs over the measured jets):

$$H_T \equiv \sum_i p_{Ti}, \qquad m_{jets} \equiv \sqrt{(\Sigma_i E_i)^2 - (\Sigma_i \vec{p}_i)^2}, \qquad y_{jets} \equiv \frac{1}{2} \ln\left(\frac{\Sigma_i E_i + \Sigma_i p_{z\,i}}{\Sigma_i E_i - \Sigma_i p_{z\,i}}\right)$$

- Differential cross sections also measured as a function of

$$z_\gamma \equiv \frac{m_{jets}}{\sqrt{s}} e^{+y_{jets}} \qquad x_A \equiv \frac{m_{jets}}{\sqrt{s}} e^{-y_{jets}}$$

ATLAS-CONF-2017-011

- Large z_γ provides access to small x_A.
- In $2 \to 2$ limit
  $x_A \to$ Bjorken-x
  $z_\gamma \to x_\gamma y$
  $H_T \to 2Q$

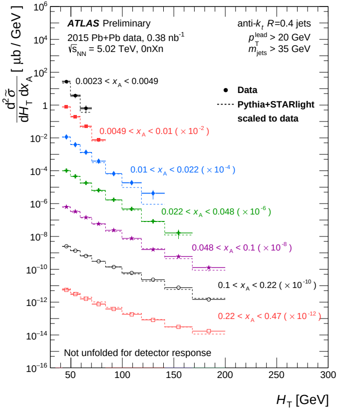

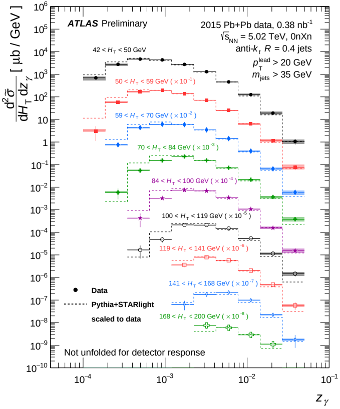

CMS-PAS-HIN-18-011

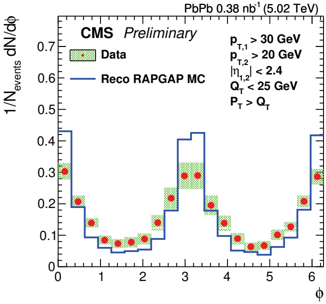

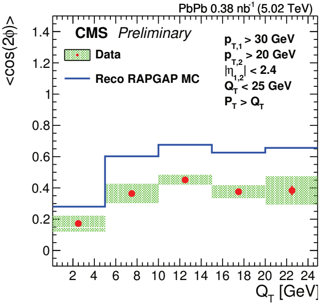

- CMS data: Pb+Pb at $\sqrt{s_{\mathrm{NN}}} = 5.02$ TeV, $\mathcal{L} = 0.38$ nb^{-1}
- Exclusive dijet photoproduction in UPC:

$$\gamma + \mathrm{Pb} \rightarrow \mathrm{jet} + \mathrm{jet} + \mathrm{Pb}$$

- Jet definition: anti-k_{T} algorithm with $R = 0.4$; leading (subleading) jet is required to have $p_{\mathrm{T}} > 30$ GeV (20 GeV); both jets with $|\eta_{\mathrm{jet}}| < 2.4$; no more jets with $p_{\mathrm{T}} > 20$ GeV.
- Dijet anisotropy is sensitive to the spatial and momentum correlations of gluons.
- Second Fourier harmonic $\langle \cos(2\phi) \rangle$ in exclusive dijets photoproduction is expected to provide insights into "elliptic gluon" dynamics - non-trivial angular correlations of the gluon Wigner distribution in the nucleus, that depend on impact parameter and gluon transverse momentum.
- ϕ is the azimutal angle between $\vec{Q}_{\mathrm{T}}$ and $\vec{P}_{\mathrm{T}}$ defined as:

$$\vec{Q}_{\mathrm{T}} = \vec{p}_{\mathrm{T},1} + \vec{p}_{\mathrm{T},2} \quad \text{and} \quad \vec{P}_{\mathrm{T}} = \frac{1}{2}(\vec{p}_{\mathrm{T},1} - \vec{p}_{\mathrm{T},2})$$

- Data are not yet corrected for detector effects!

Summary of the Snowmass UPC LoIs

- Many new results from UPC and non-UPC two-photon collisions from RHIC and LHC.
- Need for precise understanding and modeling of the WW photon source.
- Possible use as a probe of electromagnetic properties of QGP.
- Imaging of nucleus with high energy photons.
- Palarisation as a tool to access Wigner function (TMD/GDP).
- Two-photon collisions as a tool to access BSM physics.
- Photonuclear dijet production as a tool to study PDFs in nucleus.

Thank you for your attention!

Supported in part by the National Science Centre of Poland under grant UMO-2018/30/M/ST2/00395